

Article

Orthogonal Reference Surrogate Fuels for Operability Testing

Zhibin Yang, Robert Stachler and Joshua S. Heyne * 

Department of Mechanical & Aerospace Engineering, University of Dayton, Dayton, OH 45469, USA; yangz11@udayton.edu (Z.Y.); stachlerr1@udayton.edu (R.S.)

* Correspondence: jheyne1@udayton.edu

Received: 18 March 2020; Accepted: 11 April 2020; Published: 15 April 2020



Abstract: The approval and evaluation process for sustainable aviation fuels (SAF) via ASTM D4054 is both cost- and volume-intensive, namely due to engine operability testing under severe conditions. Engine operability tests of combustor under figures of merit (FOM) limit phenomena are the fuel effects on lean blowout, high-altitude relight, and cold-start ignition. One method to increase confidence and reduce volume in tiered testing is to use surrogate fuels for manipulation of properties. Key fuel performance properties (surface tension, viscosity, density) for cold-start ignition was determined prior to this study. Prior work regarding this FOM has not considered the combination of these properties. A surface tension blending rule was validated and incorporated into the jet fuel blend optimizer (JudO). A generalized surrogate calculator for N-dimensional surrogate components and features was developed. Jet fuel surrogates developed in this study were a mixture of conventional and sustainable aviation fuels instead of pure components. These surrogates suggested to be tested in this study could illuminate near worst-case effects for sustainable aviation fuel in a given configuration/rig. With those scenarios tested, we can further understand the influence on the key properties relative to cold-start ignition. This work and supporting experimental evidence could potentially lower the barrier for SAF approval processes.

Keywords: surrogate formulation; orthogonal reference surrogate fuel; operability testing; cold start ignition; sustainable aviation fuel

1. Introduction

Increases in global ambient temperature and mean sea level have had adverse effects on marine ecosystems, fishery productivity, agriculture, and the human population in coastal zones. These factors, paired with the increase in natural disasters, have led to increased volatility of the environment due to anthropocentric carbon emissions [1]. Reducing these carbon emissions through the deployment of renewable energy sources has excellent potential in the transportation sector, where aviation contributes approximately 9% of total emissions [2]. Commercial aviation must significantly reduce its greenhouse gas (GHG) impact to continue to support global mobility and commerce as NASA is predicting a 2-fold increase in passenger flights in the next decade [3]. Through the International Civil Aviation Organization (ICAO), the commercial aviation industry has adopted and defined a method to reduce the global environmental impact of air travel through Carbon Offsetting and Reduction Scheme for International Aviation (CORSIA). CORSIA sets the voluntary standards to reduce carbon emissions during Phase 1 (through 2026) and mandatory standards during Phase 2 (2027 and beyond) [4]. By the year 2050, under a CORSIA-type domestic emission policy, the demand for sustainable aviation fuel (SAF) will need to increase to more than 10% of total jet fuel consumption [5].

Commercial deployment of SAF relies on the approval and evaluation of the fuel via ASTM D4054. This specification ensures the safe usage, fungibility, performance, and compatibility of the SAF

under standard usage and severe operability conditions. Specifically, Tier 3 engine operability tests focus on fuel effects under the so-called figure-of-merit (FOM) limit phenomena, namely, lean blowout (LBO), high-altitude relight, and cold-start ignition [6–8]. Because of the broad range of potential physical and chemical properties of a new SAF, extensive combustor testing is needed to overcome uncertainty and ensure safety for FOM operability issues. Estimations for the direct testing for a candidate SAF in cost and volumes are approximated to be in the range of \$5 million and 28,000 to 115,000 gallons, respectively [9], with more contemporary approvals requiring still tens of thousands of gallons. These estimates do not include overhead costs for all parties involved in the process or the cost of supplying large quantities of potentially expensive test fuel [10]. Because of the nature of this costly and volume-intensive testing process, the National Jet Fuels Combustion Program's (NJFCP) mission is to streamline the SAF approval process and, in turn, reduce the carbon intensity of aviation transportation by ensuring a broad and diverse portfolio of SAF fuels, feedstock, and processing technologies [10–12].

Recent random forest regression (RFR) results on LBO of SAFs in four combustor rigs showed that derived cetane number (DCN) is the most significant feature importance in both the Referee Rig and toroidal jet-stirred reactor at elevated temperatures, and the second most significant feature importance in the Sheffield rig [13,14]. These three rigs show the dominance of chemical timescales near LBO, where chemical timescales are a function of the fuel chemical properties and accompanying thermodynamic conditions. However, experiments using the Honeywell auxiliary power unit (APU) show no sign of DCN affecting LBO [14]. Lack of a swirler and presence of a small pressure atomizer contribute to this difference and enhance the dominance of evaporative timescales near LBO, where evaporative timescales are a function of physical fuel properties and distillate properties. The Honeywell APU and toroidal jet-stirred reactor represent the extreme differences with Referee Rig and Sheffield Rig best representing main engine effects.

Recent RFR efforts into gas turbine combustor ignition and the relative impact of spray and volatile fuel properties indicate that the down-selected properties of viscosity, density, surface tension, vapor pressure, and specific heat capacity nearly capture the variance in ignition probability [15]. Ignition probability, a metric to determine successful ignitions, is used in gas turbine combustion where turbulence and stochasticity exist. Furthermore, viscosity, density, and surface tension have a larger impact than vapor pressure and specific heat capacity on ignition behavior for both the Referee Rig and Honeywell APU [15]. At higher fuel temperatures, surface tension is the most important property to predict relative ignitability in the Honeywell APU. The current certification process for SAF via ASTM D4054 has no specification limit for surface tension. However, surface tension is strongly and positively correlated with density, and there is a specification limit for density in all Category A fuels [11,12].

Historically, surrogates have been used for the manipulation or prescription of fuel properties to mimic the properties of target fuels. Surrogates have been used to mimic autoignition, ignition delay, extinction strain rate, and emissions. The usage of surrogate formulation to understand the combustion phenomenon has been explored by Dooley et al. [16] and Kim et al. [17,18]. Dooley et al. outlined a method for fuel-specific surrogate formulation through empirical correlation. The surrogates were designed to emulate the chemical kinetic behavior of a target, real fuel. In the work of Kim et al., two surrogates were developed with empirical correlations to emulate chemical and physical properties that affect spray and ignition within the diesel combustion process. These surrogate studies have transformed, confirmed, and in some cases transcended the fundamental understanding of combustion theory. SAF approvals could benefit from the manipulation, instead of mimicking, of properties to illustrate the complex physical competitions of properties at limit points, namely, LBO and ignition.

This work combines, modifies, and extends the work of Bell et al. [19] on the general surrogate calculator with the incorporation of recent surface tension results and the ability to create surrogates to manipulate properties without empirical correlation, and, more importantly, reports several blends of fuels that can establish a basis set for cold operability testing in aviation turbine applications. This effort further integrates NJFCP reference fuels and engine scalable blend components, instead of pure

compounds, to report orthogonal basis set fuels. Orthogonal surrogate compositions are reported from a 6-dimensional Pareto front. These compositions and properties represent the maximized variance of the reported results for hydrocarbon molecules in the jet fuel distillation range. No previous work has reported results of a comparable number of fuel properties, number of fuels, and the broader implication of their findings at once. Experimental results from testing such fuels can illustrate the maximum FOM sensitivity, aiding in the prescreening and formal evaluation of novel SAFs [10,13,20]. These tests, moreover, can be utilized to advance computational fluid dynamics modeling.

2. Materials and Methods

2.1. Materials

Thirteen fuels were used as the basis for maximizing fuel property variance. Three conventional, or Category A, fuels representing a “best” (A-1, POSF 10264), “average” (A-2, POSF 10325), and “worst” (A-3, POSF 10289) were used. Ten fuels composed of blends or neat alternative fuels were available with the relevant properties under the desired condition. The fuels utilized here were the basis of the NJFCP to investigate a wide range of chemical and physical fuel characteristics. Edwards [21,22] contains explanations of the specified reference fuels. Table A1 of Appendix A contains property information about the fuels. In Figure 1, a plot presents the fuels used in this work with key properties, revealing the variance of these properties amongst these neat blend components.

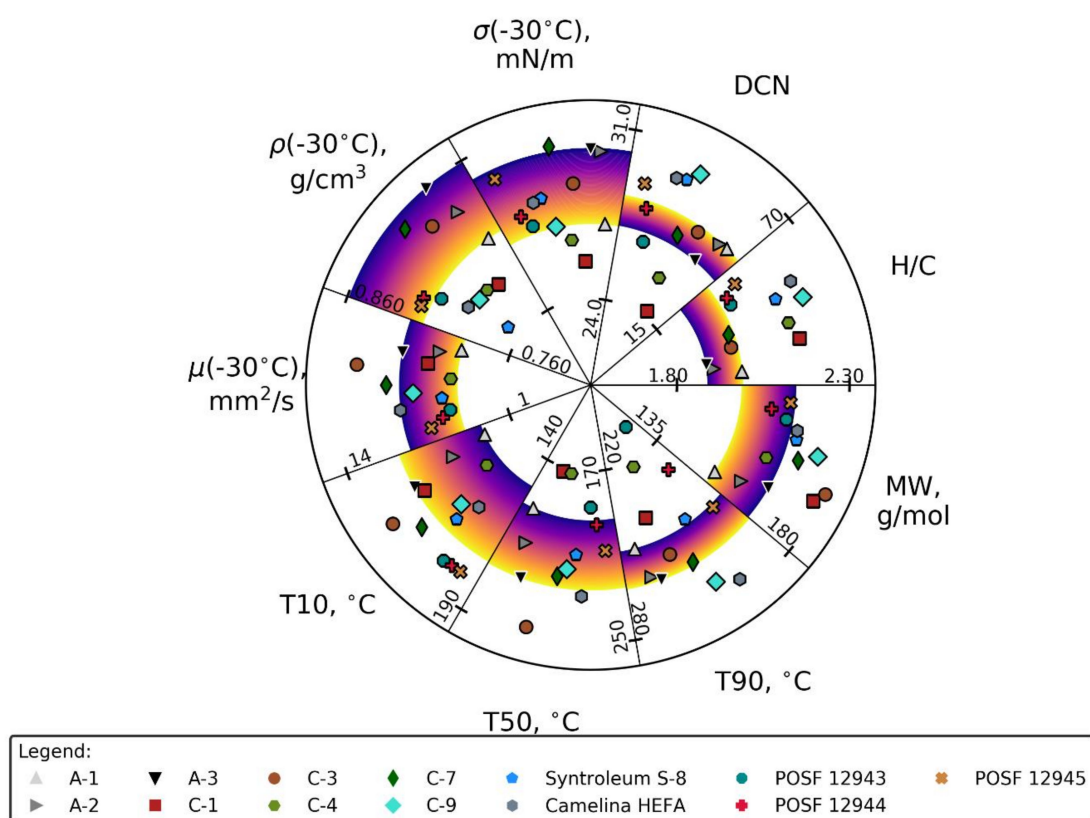


Figure 1. A plot of the 13 fuels and their respective normalized properties. Category A fuels are shown in the color gradient on the map, where yellow is the “best” case and purple is the “worst” case for each property. The rest of the fuels are plotted according to their normalized properties and respective to their marker.

2.2. Blending Rule

The blending rules used to predicting the proprieties of the optimized surrogates were applied to molecular weight (MW), atomic hydrogen-to-carbon ratio (H/C), derived cetane number (DCN),

density (ρ) at -30 °C, kinematic viscosity (μ) at -30 °C, distillation curve (T10, T50, T90), and surface tension (σ) at -30 °C. Blending rules were incorporated from the efforts of Bell et al. [19] from the general surrogate calculator, and additional validation was performed in the work of Bell et al. to ensure proper usage [19]. Surface tension blending rule for non-pure components was seldom considered and never included in the surrogate calculator. Therefore, for this effort, a surface tension blending rule will be integrated into the surrogate calculator.

The surface tension of the fuel blends was calculated using the Macleod–Sugden correlation as indicated in Equation (1) [23]. In the equation, σ_m is the surface tension of the mixture, where ρ_{Lm} and ρ_{Vm} are the liquid and vapor mixture density, respectively. $[P_{Lm}]$ and $[P_{Vm}]$ are the parachor of the liquid and vapor mixture. At low pressures, the term P_{Vm} involving vapor density could be neglected [23]. For this study, all jet fuels were blended at ambient conditions: thus, P_{Vm} is neglected. With this simplification to Equation (1), the equation can be rewritten as shown in Equation (2). Equations (3) and (4) are used to calculate the parachor of the liquid. $[P_{ij}]$ is the parachor of the mixture, where $[P_i]$ and $[P_j]$ are the parachor of pure component i and j . λ_{ij} is the binary interaction coefficient determined from experimental data; in the absence of experimental data, λ_{ij} could be set to 1. Parachor values of each fuel was calculated using surface tension, molar mass, and density of each fuel in this study. Parachor is an intermediate step before calculating surface tension of jet fuel mixture and is calculated for every intermediate step.

$$\sigma_m = [[P_{Lm}]\rho_{Lm} - [P_{Vm}]\rho_{Vm}]^n \quad (1)$$

$$\sigma_m = [[P_{Lm}]\rho_{Lm}]^n \quad (2)$$

$$[P_{Lm}] = \sum_i \sum_j x_i x_j [P_{ij}] \quad (3)$$

$$[P_{ij}] = \lambda_{ij} \frac{[P_i] + [P_j]}{2} \quad (4)$$

When n in Equation (2) is set to 4, the equation could be reduced to the Weinaug–Katz equation [24]. In this study, λ_{ij} in Equation (4) is given a value of 1 with supporting experimental material provided in Appendix A. Although in a previous application, this blending rule was used for pure component mixing, here it was used for complex jet fuels mixtures with supporting material provided in Appendix A.

2.3. Jet Fuel Blend Optimizer (JudO)

The Bell et al. general surrogate calculator [19] was shown to be effective with the aforementioned blending methods, with the exception of surface tension. However, the general surrogate calculator only minimizes overall error rather than reducing the error of each property relative to their targets individually. The JudO can optimize user-defined properties at an N -dimensional scale (with 6 dimensions explored here). The goal of this optimization is to keep other user-specified properties constant and stress certain properties to create orthogonal surrogate fuel sets. Blending rules were integrated into objective functions to achieve desired property values.

Figure 2 presents a schematic of the optimization approach, which is based on the framework of JudO [25,26]. JudO uses mole fractions of the fuel set as inputs to the optimization. All initial guesses were randomly generated, where each fuel has a chance to be assigned a value for mole fractions between 0 and 1. This strategy aids in the optimization technique to investigate a wide range of potential compositions with accompanying potential local minima, rendering an “unbiased” optimization final solution.

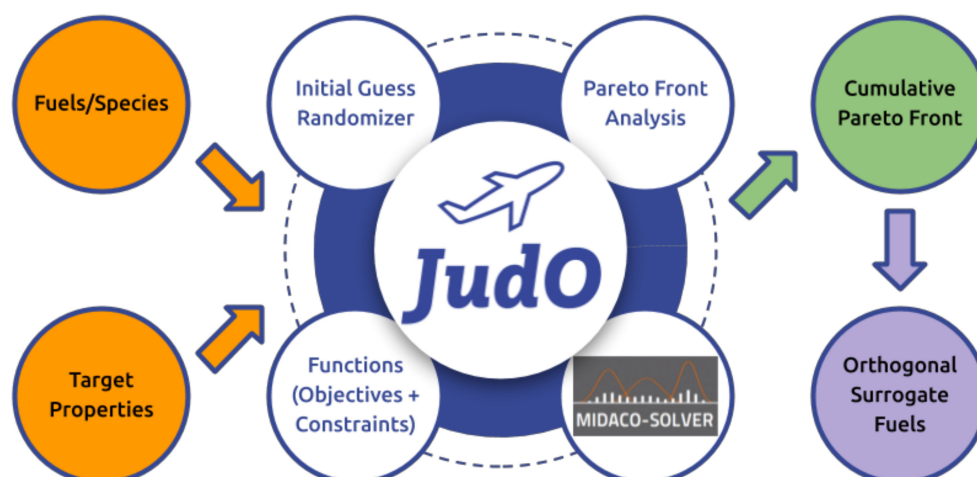


Figure 2. Schematic of the jet fuel blending optimization tool JudO, a suite centered around a computational tool called Mixed Integer Distributed Ant Colony Optimization (MIDACO) [27], which is implemented to optimize a user-specified fuel set (conventional and alternative jet fuels) of varying properties with specific “design parameters and target properties” (molecular weight—MW, hydrogen-to-carbon ratio—H/C, derived cetane number—DCN, density, kinematic viscosity, distillation curve, and surface tension) to illuminate Pareto front compromises for the fuels considered here.

Once the initial guess is determined, a Mixed Integer Distributed Ant Colony Optimization (MIDACO) solver [27] starts to optimize the mole fractions based on the given random initial guess with supplied objective and constraint functions. The objective functions were evaluated on the l2 norm and normalized to A-2 values. MIDACO is a commercially available numerical high-performance solver that uses ant colony optimization with multiple objective functions to obtain a near-global optimum solution. An advantage of using this solver is the derivative-free, evolutionary hybrid algorithm that treats the objective and constraint functions as a “black-box which may contain critical function properties like non-linearity, non-convexity, discontinuities or even stochastic noise” [27]. A disadvantage of these types of genetic algorithm optimizations is that they do not guarantee convergence and unique Pareto front solutions. Hence multiple initial guesses were employed to unbias a final cumulative Pareto front from initializations.

When the optimization is complete with the supplied compositions, functions, and thus, fuel mixture properties, JudO outputs a range of Pareto front mole fractions for that particular initial guess composition. Those Pareto front solutions are then compiled to form a cumulative Pareto front, which is a culmination of all Pareto solutions from the initial guesses. For each of the three scenarios outlined later, 10,000 initial guesses were used to generate numerous individual Pareto fronts and one final cumulative Pareto front for each scenario. With the nature of 6-dimensional optimization, more than one Pareto front was generated for each initial guess. Down-selection for each scenario is then performed on the cumulative Pareto front space with discrete optimization to capture the broadest combination of relative variance amongst viscosity, density, and surface tension. Orthogonal surrogate fuels were then determined via down-selection from the compiled solutions presented in the cumulative Pareto front. Orthogonality in this study was focused only on the three properties of interest (surface tension, density, viscosity).

2.4. Orthogonal Array Testing

For this study and due to the inherent multidimensionality pertaining to the fuel properties, blending rules, and multi-component fuels themselves, a design of experiments approach is needed. Taguchi’s orthogonal array testing was utilized to maximize the variance in results during combustor FOM testing and to minimize the number of tests [28,29]. Orthogonal arrays can be considered as a template for multivariable experiments where the columns correspond to the variables, the elements

in the columns represent the test levels of the variables, and the rows correspond to the test run [28]. This effort involves three variables (surface tension, viscosity, density) and two levels for each variable (larger than A-2 value, smaller than A-2 value), A-2 is utilized here because it represents the ‘average’ conventional jet fuel. In a traditional sense, the orthogonality is achieved with six surrogate sets, where each surrogate would keep all properties the same with A-2 and maximize/minimize one property of interest (surface tension, viscosity, density). However, with Taguchi’s orthogonal array testing, orthogonality can be achieved with four surrogate sets instead. Four scenarios were generated in Table 1 according to the appropriate variable and level based on orthogonal array testing [28,29].

Table 1. Orthogonal array testing.

| Scenarios | σ (−30 °C), mN/m | μ (−30 °C), mm ² /s | ρ (−30 °C), kg/L | Surrogate |
|-----------|-------------------------|------------------------------------|-----------------------|-----------|
| Reference | 30.0 | 6.1 | 0.837 | A-2 |
| [1] | ↓ | ↓ | ↓ | 1 |
| [2] | ↓ | ↑ | ↑ | 2 |
| [3] | ↑ | ↓ | ↑ | 3 |
| [4] | ↑ | ↑ | ↓ | 4 |

3. Results and Discussions

This study focuses on creating surrogate fuels with orthogonal properties using real fuels as surrogate components for scaled rig testing. Four scenarios were reported to elucidate the potential operability variance by mid-distillate hydrocarbons in aviation gas turbine engines, see scenarios reported in Table 1. For each orthogonal array test scenario, 10,000 random initial compositional guesses to unbiased solutions and the corresponding Pareto solutions were used to generate the cumulative Pareto front. Figures 3–6 consists of scatter plots and histograms of Pareto front solutions illustrating converged probability densities and relative opportunities for property variance. Each scatter plot consists of calculated properties. Each of the dots on the scatter plots represents one of the possible best solutions found by JudO. The purple dashed line represents the properties of A-2. A surrogate was selected using orthogonal array testing, from the total set of solutions presented initially and represented by the orange star. The surrogates were selected to minimize or maximize the properties of density, viscosity, and surface tension relative to A-2, according to the four scenarios. Other properties were intended to be as close to the A-2 values as possible using the other objective functions in this optimization. Although the selected surrogate might not have the minimum values of the solution space, the multi-dimensionality concerning all the properties suggests the largest variance happens at that point.

Down selected surrogate fuels for each of the scenarios are presented in Table 2 with their respective properties, where Figures 3–6 identify the mole fractions and volume fractions of each surrogate. Four surrogate fuels based on the scenario results were then blended and measured at −30 °C for viscosity and density. No error beyond experimental confidence intervals was observed between the measured and calculated density at −30 °C for the four blended fuels. Viscosity measurements illuminated favorable error relative to the predicted values as additional variance beyond the calculated variance was observed. Unfortunately, under the lab’s current experimental capabilities, surface tension measurements are limited to near room temperature.

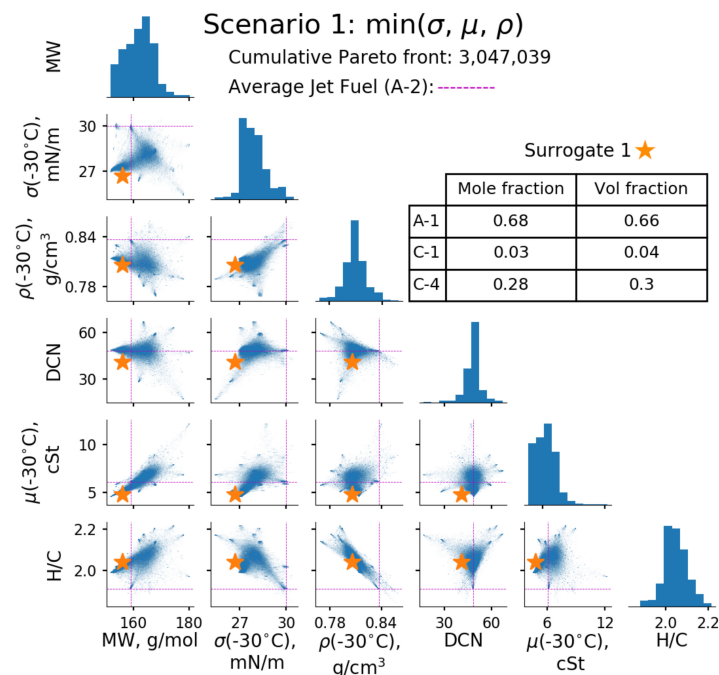


Figure 3. Cumulative Pareto solutions for scenario 1 with combinations of optimized properties on histograms and scatter plots with other properties. Scatter plots consist of calculated properties with respect to each other. Each dot on a scatter plot represents one of the possible best solutions found using the jet fuel blending optimization tool JudO. The dashed line indicates the properties of A-2, and the orange star represents the properties of surrogate 1 with respect to the cumulative Pareto solutions.

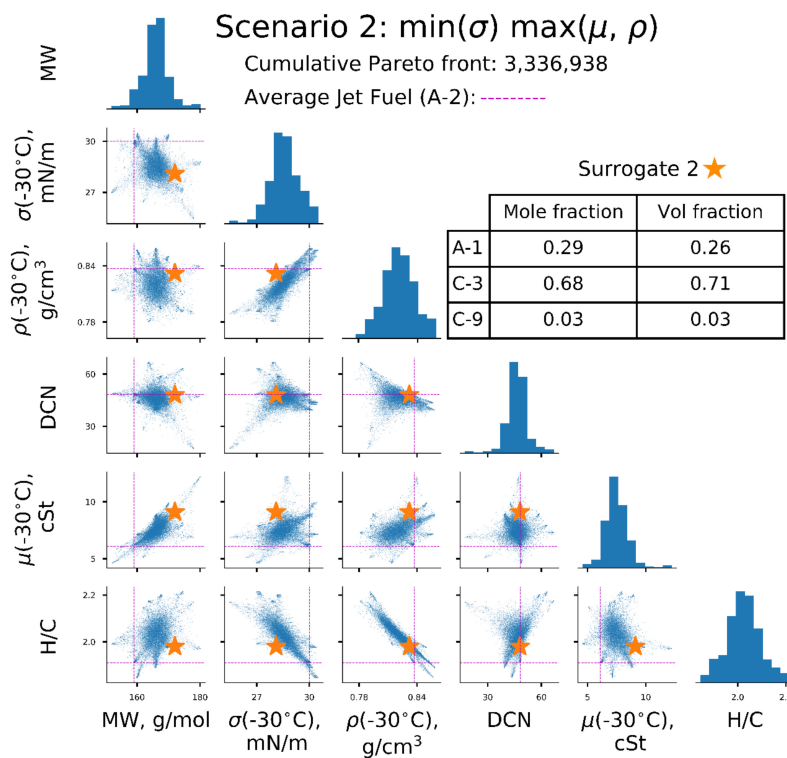


Figure 4. Cumulative Pareto solutions for scenario 2 with the chosen surrogate, indicated with the orange star. Refer to Figure 3 for plot details.

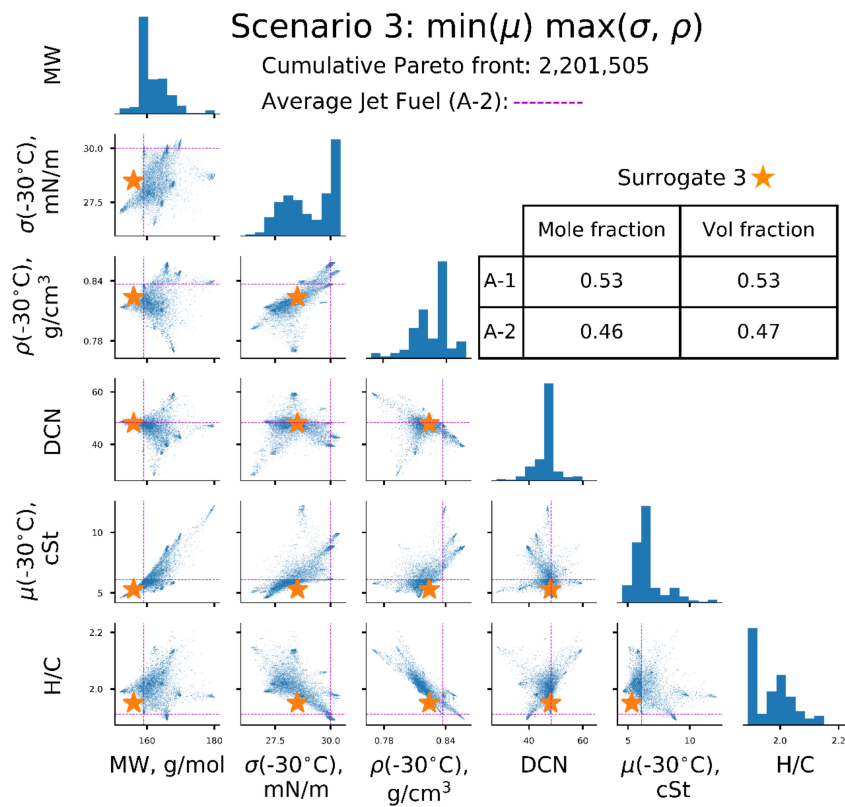


Figure 5. Cumulative Pareto solutions for scenario 3 with the chosen surrogate, indicated with the orange star. Refer to Figure 3 for plot details.

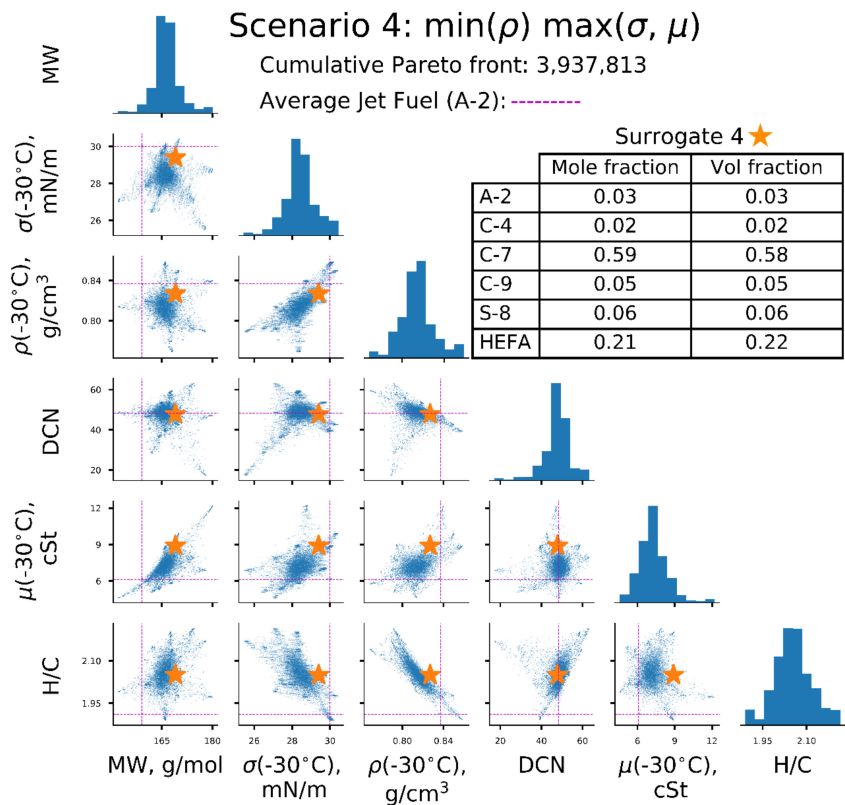


Figure 6. Cumulative Pareto solutions for scenario 4 with the chosen surrogate, indicated with the orange star. Refer to Figure 3 for plot details.

Table 2. Properties of orthogonal fuels for all scenarios.

| Property | Scenario | | | | |
|------------------------------------|---------------|---|--|--|---|
| | A-2 Reference | Surrogate 1 min (σ , μ , ρ) | Surrogate 2 min (σ), max (μ , ρ) | Surrogate 3 min (μ), max (σ , ρ) | Surrogate 4 min(ρ), max (σ , μ) |
| MW, g/mol | 159 | 156 | 172 | 156 | 169 |
| σ (−30 °C), mN/m | 30.0 | 26.7 | 28.1 | 28.5 | 29.4 |
| ρ (−30 °C), kg/L | 0.837 | 0.806/ 0.806 * | 0.832/ 0.832 * | 0.824/ 0.824 * | 0.827/ 0.826 * |
| μ (−30 °C), mm ² /s | 6.1 | 4.8/ 4.5 * | 9.1/ 10.3 * | 5.3/ 5.2 * | 8.9/ 8.5 * |
| DCN | 48 | 41 | 48 | 48 | 48 |
| H/C | 1.91 | 2.04 | 1.98 | 1.95 | 2.05 |
| T10, °C | 160 | 151 | 175 | 154 | 173 |
| T50, °C | 209 | 186 | 231 | 201 | 218 |
| T90, °C | 260 | 241 | 254 | 254 | 262 |
| | | Mole fraction | | | |
| A-1 | | 0.68 | 0.29 | 0.53 | |
| A-2 | 1.00 | | | 0.46 | 0.03 |
| C-1 | | 0.03 | | | |
| C-3 | | | 0.68 | | |
| C-4 | | 0.28 | | | 0.02 |
| C-7 | | | | | 0.59 |
| C-9 | | | 0.03 | | 0.05 |
| S-8 | | | | | 0.06 |
| HEFA | | | | | 0.21 |

* Properties measured at −30 °C.

Figure 3 displays the total of 3,047,039 results of scenario 1. Here, the resulting surrogate, Surrogate 1, was intended to have the lowest surface tension, viscosity, and density. Compositionally, Surrogate 1 consists primarily of 68% A-1 and 28% C-4, where A-1 is the “best” jet fuel, with all three properties lower than that of A-2, and C-4 has the second-lowest surface tension and relatively low viscosity and density. C-1 has the lowest surface tension; however, with relatively high viscosity, it was not considered in the solution of Surrogate 1. Figure 4 illuminates scenario 2, which minimizes surface tension and maximizes viscosity and density. Each of the 3,336,938 possible best solutions is shown on the scatter plots. The orange star represents Surrogate 2, which was the best solution for this scenario. This mixture consists of 29% A-1 and 68% C-3, where C-3 has the highest viscosity and relatively high density. Figure 5 shows 2,201,505 solutions for scenario 3 and, like the previous figures, indicates the best solution for Surrogate 3 by the orange star. The goal of Surrogate 3 was to minimize viscosity and maximize surface tension and density. Surrogate 3 consists of 53% A-1 and 46% A-2, where A-2 is the target fuel of this study. Figure 6 reports 3,937,813 solutions for scenario 4, and the objective for Surrogate 4 was to minimize density and maximize surface tension and viscosity. The selected surrogate consisted of a six-component mixture, very different from the other solutions: 3% A-2, 2% C-4, 59% C-7, 5% C-9, 5% Syntroleum S-8, and 21% Camelina HEFA. This is because minimizing density, while maximizing surface tension was difficult with the fuels selected for this work. The majority of the fuels selected in this effort had positive correlations between surface tension and density, making it difficult to minimize density while maximizing surface tension. If a larger variance is needed, then more novel fuel, solvents, and neat molecules need to be integrated into JudO. Neat molecules, such as alkylbenzenes, where surface tension and density are not positively correlated would aid JudO in capturing additional variance; thus, surface tension and density can be more orthogonalized. Solvents such as Aromatics 100 and 150, for example, could aid in adding more extreme high surface tensions and densities, and low viscosities.

4. Conclusions

In conclusion, the current approval and evaluation process of SAFs are both costly and volume-intensive, for fuels that do not qualify for Fast Track (ASTM D4054 Annex A4). Extensive combustor testing is needed to overcome the uncertainty and ensure safety under FOM limit phenomena. Surrogates that mimic jet fuel properties have been used historically to understand combustion phenomena, while here we report potentially worst case fuel compositions. Previous efforts from the NJFCP program have shown that certain fuel properties (σ , μ , and ρ) have more of an impact on predicting ignition probabilities [14,15,30]. SAF approval could benefit from the manipulation instead of mimicking surrogate properties to illustrate the complex physical competition of properties. Three worst case fuel property scenarios are reported that would bound combustion operability effects and help to build confidence and building a detailed model for future analysis of the combustor ignition problem. A generalizable surrogate calculator with the incorporation of recent surface tension results and the ability to manipulate properties at an N-dimensional scale is created. Four scenarios were explored computationally to create four orthogonal surrogate sets that maximize variance in the specified fuel properties. Those four orthogonal surrogates were later measured for the given properties of interest at desired temperature to confirm the predicted values. In this study, surrogate compositions were able to extend the work of Kim et al. [17] and Dooley et al. [16] to create scalable surrogates without empirical correlation and manipulating properties more important to aviation combustor FOM operability. Now surrogates can be developed using full distillate conventional fuels and SAF instead of pure components. The surrogate fuels suggested to be tested could illuminate the worst-case effects for an alternative jet fuel in a given configuration/rig, which aids in bounding the maximum impact of fuels on these critical safety metrics. This work and supporting experimental evidence could lower the barrier for SAF approval processes and facilitate the achievement of the carbon reduction goals. In future research, more properties need to be added to JudO to cover more FOMs, and more novel fuels, solvents, and neat molecules need to be considered for integration in this tool to achieve greater variance in properties than currently estimated.

Author Contributions: Conceptualization, Z.Y.; Methodology, Z.Y.; Software, Z.Y. and R.S.; Validation, Z.Y.; Formal analysis, Z.Y.; Investigation, Z.Y.; Resources, Z.Y.; Data curation, Z.Y.; Writing—Original draft preparation, Z.Y.; Writing—Review and editing, R.S. and J.S.H.; Visualization, Z.Y.; Supervision, J.S.H.; Project administration, J.S.H.; Funding acquisition, J.S.H. All authors have read and agreed to the published version of the manuscript.

Funding: This research was funded by U.S. Federal Aviation Administration Office of Environment and Energy through ASCENT, the FAA Center of Excellence for Alternative Jet Fuels and the Environment, Project 34 through FAA Award Number 13-CAJFE-UD-18 under the supervision of Cecilia Shaw and Anna Oldani.

Acknowledgments: We would also like to acknowledge Tim Edwards, Katherine Opacich, and Shane Kosir for their support in this research effort, which would not have been possible without their help.

Conflicts of Interest: The authors declare no conflict of interest.

Abbreviations

| | |
|--------|---|
| APU | Auxiliary Power Unit |
| CORSIA | Carbon Offsetting and Reduction Scheme for International Aviation |
| DCN | Derived Cetane Number (ASTM D6890) |
| FOM | Figure of Merit |
| GHG | Greenhouse Gas |
| H/C | Atomic Hydrogen-to-Carbon Ratio |
| ICAO | International Civil Aviation Organization |
| JudO | Jet Fuel Blend Optimizer |
| LBO | Lean Blowout |
| MIDACO | Mixed Integer Distributed Ant Colony Optimization |
| MW | Molecular Weight, g/mol |
| NJFCP | National Jet Fuels Combustion Program |
| RFR | Random Forest Regression |
| SAF | Sustainable Aviation Fuel |

Appendix A

Contained in this appendix are additional figures and tables from this research effort. Figure A1 displays the surface tension accuracy of calculated values relative to measurement. Table A1 presents the fuels used with the properties of MW, H/C ratio, derived cetane number (DCN), T10, T50, and T90. Surface tension, viscosity, and density were predicted at $-30\text{ }^{\circ}\text{C}$.

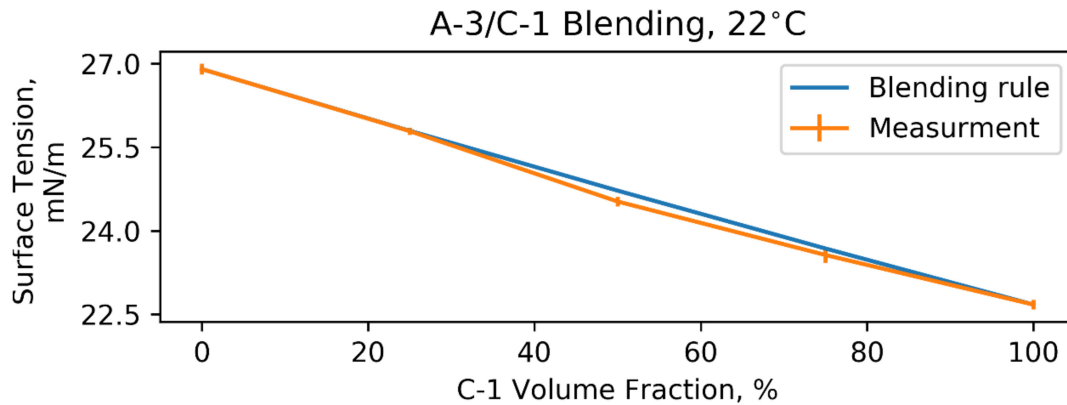


Figure A1. Surface tension blending rule validation. Error bar represent 95 percent confidence interval.

Table A1. All properties of the fuels used in this study.

| Fuel, POSF | MW | H/C | DCN | Surface Tension $-30\text{ }^{\circ}\text{C}$ * (σ), mN/m | Viscosity $-30\text{ }^{\circ}\text{C}$ * (ν), mm ² /s | Density $-30\text{ }^{\circ}\text{C}$ * (ρ), kg/m ³ | T10, $^{\circ}\text{C}$ | T50, $^{\circ}\text{C}$ | T90, $^{\circ}\text{C}$ |
|----------------------|-----|------|------|--|---|---|-------------------------|-------------------------|-------------------------|
| A-1, 10264 | 152 | 1.99 | 48.8 | 27.1 | 4.6 | 0.814 | 149 | 193 | 249 |
| A-2, 10325 | 159 | 1.91 | 48.3 | 30.0 | 6.1 | 0.837 | 160 | 209 | 260 |
| A-3, 10289 | 166 | 1.89 | 39.2 | 30.1 | 8.9 | 0.859 | 174 | 225 | 262 |
| C-1, 11498 | 178 | 2.17 | 17.1 | 25.5 | 6.9 | 0.789 | 172 | 172 | 240 |
| C-3, 12341 | 180 | 1.97 | 47.0 | 28.7 | 12.2 | 0.840 | 185 | 246 | 255 |
| C-4, 12344 | 162 | 2.15 | 28.0 | 26.4 | 5.1 | 0.792 | 153 | 172 | 222 |
| C-7, 12973 | 170 | 1.98 | 42.6 | 30.3 | 9.9 | 0.851 | 179 | 220 | 261 |
| C-9, 12968 | 174 | 2.22 | 63.3 | 27.1 | 7.9 | 0.791 | 166 | 216 | 271 |
| Syntroleum S-8, 5018 | 168 | 2.14 | 59.7 | 28.3 | 5.7 | 0.769 | 170 | 209 | 247 |
| Camelina HEFA, 7720 | 168 | 2.20 | 58.9 | 28.3 | 9.0 | 0.794 | 163 | 228 | 275 |
| 12943 | 164 | 2.02 | 36.1 | 27.4 | 5.3 | 0.810 | 181 | 187 | 209 |
| 12944 | 160 | 2.02 | 46.4 | 27.9 | 5.9 | 0.819 | 181 | 195 | 230 |
| 12945 | 165 | 2.01 | 54.0 | 29.7 | 6.9 | 0.818 | 181 | 207 | 250 |

* Properties are predicted at $-30\text{ }^{\circ}\text{C}$.

References

- Neumann, B.; Vafeidis, A.T.; Zimmermann, J.; Nicholls, R.J. Future Coastal Population Growth and Exposure to Sea-Level Rise and Coastal Flooding—A Global Assessment. *PLoS ONE* **2015**, *10*, e0118571. [[CrossRef](#)] [[PubMed](#)]
- Office of Transportation and Air Quality Fast Facts, U.S. *Transportation Sector Greenhouse Gas Emissions 1990–2017*; Office of Transportation and Air Quality Fast Facts U.S.: Washington, DC, USA, 2019.
- NASA. *NASA Update FAA ASCENT Meeting*; NASA: Washington, DC, USA, 2018.
- IATA. *Carbon Offsetting and Reduction Scheme for International Aviation (CORSA): Fact Sheet*; IATA: Montreal, QC, Canada, 2016.
- Chao, H.; Buyung, D.; Delaurentis, D.; Stechel, E.B. Carbon off setting and reduction scheme with sustainable aviation fuel options: Fleet-level carbon emissions impacts for U.S. airlines. *Transp. Res. Part D* **2020**, *75*, 42–56. [[CrossRef](#)]
- Rock, N.; Emerson, B.; Seitzman, J.; Lieuwen, T. Liquid Fuel Property Effects on Lean Blowout in an Aircraft Relevant Combustor. *J. Eng. Gas Turbines Power* **2019**, *141*, 1–13. [[CrossRef](#)]
- Lefebvre, A.H. Fuel Effects On Gas Turbine Combustion. *Int. J. Turbo Jet Engines* **2004**, *3*, 3. [[CrossRef](#)]
- Stachler, R.; Heyne, J.; Stouffer, S.; Miller, J. Lean Blowoff in a Toroidal Jet-Stirred Reactor: Implications for Alternative Fuel Approval and Potential Mechanisms for Autoignition and Extinction. *Energy Fuels* **2020**. [[CrossRef](#)]

9. Rumizen, M. *D4054 Clearinghouse 2018*; CAAFI(Commercial Aviation Alternative Fuels Initiative): Washington, DC, USA, 2018.
10. Colket, M.; Heyne, J.; Rumizen, M.; Gupta, M.; Edwards, T.; Roquemore, W.M.; Andac, G.; Boehm, R.; Lovett, J.; Williams, R.; et al. Overview of the National Jet Fuels Combustion Program. *AIAA J.* **2017**, *55*, 1087–1104. [[CrossRef](#)]
11. Heyne, J.S.; Colket, M.B.; Gupta, M.; Jardines, A.; Moder, J.P.; Edwards, J.T.; Roquemore, M.; Li, C.; Rumizen, M. Year 2 of the National Jet Fuels Combustion Program: Towards a Streamlined Alternative Jet Fuels Certification Process. In Proceedings of the 55th AIAA Aerospace Sciences Meeting, Grapevine, TX, USA, 9–13 January 2017; pp. 1–14.
12. Heyne, J.S.; Peiffer, E.; Colket, M.B.; Jardines, A.; Shaw, C.; Moder, J.P.; Roquemore, W.M.; Edwards, J.T.; Li, C.; Rumizen, M.; et al. Year 3 of the National Jet Fuels Combustion Program: Practical and Scientific Impacts of Alternative Jet Fuel Research. In Proceedings of the 2018 AIAA Aerospace Sciences Meeting, Kissimmee, FL, USA, 8–10 January 2018.
13. Peiffer, E.E.; Heyne, J.S. Characteristic Timescales for Lean Blowout of Alternative Jet Fuels in Four Combustor Rigs. In Proceedings of the 2018 Joint Propulsion Conference, Cincinnati, OH, USA, 9–11 July 2018.
14. Peiffer, E.E.; Heyne, J.S.; Colket, M. Sustainable Aviation Fuels Approval Streamlining: Auxiliary Power Unit Lean Blowout Testing. *AIAA J.* **2019**, *57*, 4854–4862. [[CrossRef](#)]
15. Opacich, K.C.; Heyne, J.S.; Peiffer, E.; Stouffer, S.D. Analyzing the Relative Impact of Spray and Volatile Fuel Properties on Gas Turbine Combustor Ignition in Multiple Rig Geometries. *AIAA Sci. Technol. Forum* **2019**, *1*, 1434.
16. Dooley, S.; Won, S.H.; Chaos, M.; Heyne, J.; Ju, Y.; Dryer, F.L.; Kumar, K.; Sung, C.J.; Wang, H.; Oehlschlaeger, M.A.; et al. A jet fuel surrogate formulated by real fuel properties. *Combust. Flame* **2010**, *157*, 2333–2339. [[CrossRef](#)]
17. Kim, D.; Martz, J.; Violi, A. A surrogate for emulating the physical and chemical properties of conventional jet fuel. *Combust. Flame* **2014**, *161*, 1489–1498. [[CrossRef](#)]
18. Kim, D.; Martz, J.; Abdul-Nour, A.; Yu, X.; Jansons, M.; Violi, A. A six-component surrogate for emulating the physical and chemical characteristics of conventional and alternative jet fuels and their blends. *Combust. Flame* **2017**, *179*, 86–94. [[CrossRef](#)]
19. Bell, D.; Heyne, J.S.; Won, S.H.; Dryer, F.; Haas, F.M.; Dooley, S. On the Development of General Surrogate Composition Calculations for Chemical and Physical Properties. In Proceedings of the 55th AIAA Aerospace Sciences Meeting, Grapevine, TX, USA, 9–13 January 2017; pp. 1–5.
20. Ruan, H.; Qin, Y.; Heyne, J.; Gieleciak, R.; Feng, M.; Yang, B. Chemical compositions and properties of lignin-based jet fuel range hydrocarbons. *Fuel* **2019**, *256*, 115947. [[CrossRef](#)]
21. Edwards, J.T.; Shafer, L.M.; Klein, J.K. *U.S. Air Force Hydroprocessed Renewable Jet (HRJ) Fuel Research*; Air Force Research Laboratory: Dayton, OH, USA, 2013.
22. Edwards, T. Reference Jet Fuels for Combustion Testing. In Proceedings of the 55th AIAA Aerospace Sciences Meeting, Grapevine, TX, USA, 9–13 January 2017; pp. 1–58.
23. Poling, B.; Prausnitz, J.; O'Connell, J. *The Properties of Gases and Gas Mixtures*; McGraw-Hill: New York, NY, USA, 2000; ISBN 0071499997.
24. Weinaug, C.F.; Katz, D.L. Surface Tensions of Methane-Propane Mixtures. *Ind. Eng. Chem.* **1943**, *35*, 239–246. [[CrossRef](#)]
25. Kosir, S.T.; Behnke, L.; Heyne, J.S.; Zabarnick, S.; Flora, G.; Denney, R.K.; Tai, J.; Gupta, M. Improvement in Jet Aircraft Operation with the Use of High-Performance Alternative Drop-in Fuels in Conventional Fuels. *AIAA SciTech Forum* **2019**, *1*, 0993.
26. Flora, G.; Kosir, S.; Heyne, J.; Zabarnick, S.; Gupta, M. Properties Calculator and Optimization for Drop-in Alternative Jet Fuel Blends. *AIAA SciTech Forum* **2019**, *1*, 2368.
27. Schlueter, M.; Erb, S.O.; Gerdts, M.; Kemble, S. MIDACO on MINLP Space Applications. *Adv. Space Res.* **2013**, *51*, 1116–1131. [[CrossRef](#)]
28. Lagergren, E.S.; Filliben, J.J. Taguchi Vs Orthogonal Arrays Are Classical Designs of Experiments. *J. Res. Natl. Inst. Stand. Technol.* **1991**, *96*, 577.

29. TSUI, K.-L. An Overview of Taguchi Method and Newly Developed Statistical Methods for Robust Design. *IIE Trans.* **1992**, *24*, 44–57. [[CrossRef](#)]
30. Heyne, J.S.; Opacich, K.C.; Peiffer, E.E.; Colket, M. The effect of chemical and physical fuel properties on the approval and evaluation of alternative jet fuels. In Proceedings of the 11th U.S. National Combustion Meeting, Combustion Institute, Pasadena, CA, USA, 24–27 March 2019.



© 2020 by the authors. Licensee MDPI, Basel, Switzerland. This article is an open access article distributed under the terms and conditions of the Creative Commons Attribution (CC BY) license (<http://creativecommons.org/licenses/by/4.0/>).